

Comparative Study of Nano-Cylindrical Waveguide and Buried-SiO2 Apertures in Blue InGaN VCSELs

Downloaded from: https://research.chalmers.se, 2025-11-29 02:11 UTC

Citation for the original published paper (version of record):

Sharma, L., Persson, L., Ciers, J. et al (2025). Comparative Study of Nano-Cylindrical Waveguide and Buried-SiO2 Apertures in Blue InGaN VCSELs. Proceedings of the International Conference on Numerical Simulation of Optoelectronic Devices, NUSOD, 25: 131-132. http://dx.doi.org/10.1109/NUSOD64393.2025.11199551

N.B. When citing this work, cite the original published paper.

© 2025 IEEE. Personal use of this material is permitted. Permission from IEEE must be obtained for all other uses, in any current or future media, including reprinting/republishing this material for advertising or promotional purposes, or reuse of any copyrighted component of this work in other works.

Comparative Study of Nano-Cylindrical Waveguide and Buried-SiO₂ Apertures in Blue InGaN VCSELs

Lakshminarayan Sharma, Lars Persson, Joachim Ciers, and Åsa Haglund

Department of Microtechnology and Nanoscience

Chalmers University of Technology,

41296 Gothenburg, Sweden

sharmal@chalmers.se

Abstract—We study transverse mode control in InGaN-based blue vertical-cavity surface-emitting lasers (VCSELs) by investigating the most common index-guiding structure which is an etched nano-cylinder with and without a refill of SiO₂. Using 2–8 μ m wide aperture diameters, we evaluate key performance metrics—threshold material gain (g_{th}) and modal discrimination. The etched aperture with a 5 nm etch depth exhibited the lowest threshold material gain among the designs studied. Notably, this configuration showed the smallest increase in threshold material gain when the aperture diameter was reduced from 8 μ m to 2 μ m. Furthermore, when decreasing the aperture from 8 μ m to 4 μ m, the g_{th} for the fundamental LP₀₁ mode increased by just 95 cm⁻¹, while still achieving a high modal discrimination of 395 cm⁻¹. These results highlight the ability of the etched aperture to maintain low loss and strong mode selectivity over a practical range of aperture sizes.

I. INTRODUCTION

A truly single-mode VCSEL operates only in the fundamental mode, producing a near-Gaussian beam with superior spectral purity, and low divergence. These properties are critical for various applications such as underwater optical wireless communication, smart glasses, adaptive laser headlights, and atomic clocks.

Lateral optical and current confinement have been achieved through various aperture design approaches in InGaN VC-SELs. Such as silicon diffusion [1], air-gap aperture formed by photoelectrochemical etching [2], buried SiO₂ layer [3], and etched-passivated nano-cylindrical aperture [4].

Kuramoto et al. [4] and Terao et al. [5] have experimentally demonstrated single-mode operation in blue-emitting VCSELs using nano-cylindrical apertures with diameters of 3.3 μ m and 4 μ m, respectively. These results underscore the effectiveness of the nano-cylindrical design in promoting single-mode operation while maintaining a relatively simple and fabrication-friendly structure.

In this paper, we simulated the threshold material gain and modal discrimination of blue InGaN VCSELs having two aperture designs for lateral index guiding; an etched nanocylinder with and without a refill of SiO_2 . The etched aperture had an etch depth of 5 or 10 nm and the SiO_2 refilled had an etch depth of 20 nm that was filled up with 20 nm of SiO_2 .

This project has received funding from the European Innovation Council (EIC) under grant agreement 101130710 funded by the European Union.

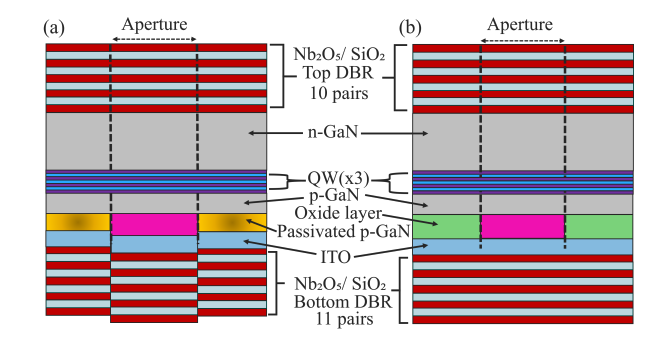


Fig. 1. Schematic of the the simulated VCSEL structure (a) with a passivated nano-cylindrical waveguide aperture and (b) with a buried SiO_2 aperture.

The studied aperture diameters were $2 \mu m$, $4 \mu m$, $6 \mu m$, and $8 \mu m$.

II. DEVICE SIMULATION DESIGN AND PARAMETERS

The VCSEL structure was simulated in Comsol multiphysics, using the finite element eigenfrequency solver. The schematic of the two aperture designs is shown in Figure 1. The VCSEL structure consists of a 10 λ cavity sandwiched in between 10 top and 11 bottom distributed Bragg reflectors (DBRs) of SiO $_2$ and Nb $_2$ O $_5$. The DBR pairs were assumed to have zero absorption loss whereas the absorption coefficient for the quantum well barrier was 3 cm $^{-1}$, GaN 1 cm $^{-1}$, p-GaN 75 cm $^{-1}$ and ITO 1000 cm $^{-1}$.

III. RESULTS AND DISCUSSION

The modal discrimination was calculated as the difference in the threshold material gain (g_{th}) for the fundamental mode (LP_{01}) and the next higher order modes $(LP_{11} \text{ or } LP_{02})$. Figure 2 shows the variation in g_{th} for LP_{01} as a function of the aperture diameter. As expected, g_{th} increases with decreasing aperture size due to increased diffraction loss, especially for aperture diameters below $4\,\mu\text{m}$. The effective index difference [6] (Δn_{eff}) between the central aperture region and the periphery region as shown in Figure 1 is 6.11 x 10^{-3} for a 5 nm etch, 12.27×10^{-3} for 10 nm etch and 8.16×10^{-3} for a 20 nm etched structure filled up with SiO_2 . A larger Δn_{eff} leads to an enhancement in the mode confinement, but at the expense of an increase in the diffraction losses. The 5 nm

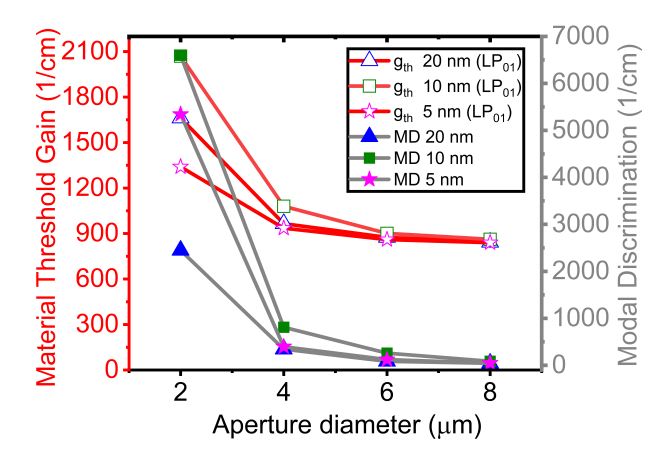


Fig. 2. Simulated impact of the aperture diameter on threshold material gain $(g_{\rm th})$ for LP₀₁ in red and modal discrimination in gray for 20 nm buried SiO₂ aperture and nano-cylindrical aperture with 10 nm and 5 nm etch depth.

nano-cylindrical waveguide, with the smallest Δn_{eff} , shows the lowest g_{th} , while the 10 nm design, with the largest Δn_{eff} , exhibits the highest g_{th} across all aperture sizes. Figure 2 also presents the corresponding modal discrimination values for each structure as a function of the aperture diameter. The 5 nm etched nano-cylindrical waveguide design exhibited superior modal discrimination, particularly for smaller aperture diameters. For an aperture diameter of $2 \mu m$, the 5 nm nano-cylindrical waveguide structure showed a modal discrimination of $5340 \,\mathrm{cm}^{-1}$ and g_{th} of $1340 \,\mathrm{cm}^{-1}$, while the 20 nm SiO₂ buried structure showed values of 2448 cm⁻¹ and 1661 cm⁻¹. The high modal discrimination reflects strong lateral confinement, which suppresses higher-order modes but also increases diffraction losses, raising the threshold gain. A $4 \mu m$ aperture diameter device with 5 nm etch shows a good trade-off between high modal discrimination (395 cm⁻¹) and low threshold material gain (935 cm $^{-1}$). The 20 nm SiO₂ configuration was equally good in terms of single-mode performance with a threshold material gain of 965 cm⁻¹ and modal discrimination of $345 \,\mathrm{cm}^{-1}$.

Figure 3 presents a tolerance analysis for the $4\,\mu\rm m$ aperture case reflecting realistic fabrication deviations. The calculated $g_{\rm th}$ remained relatively stable, with values of $920\,{\rm cm}^{-1}$ for a 4 nm etch depth and $956\,{\rm cm}^{-1}$ for 6 nm. The corresponding modal discrimination values were $339\,{\rm cm}^{-1}$ for a 4 nm etch depth and $473\,{\rm cm}^{-1}$ for 6 nm - sufficient to favor LP₀₁ over higher order modes and maintain single mode operation.

The g_{th} values for the constant 20 nm p-GaN etch with deposited SiO₂ thickness equal to 19 nm is $952\,\mathrm{cm}^{-1}$ and for 21 nm is $986\,\mathrm{cm}^{-1}$. The corresponding modal discrimination values were $376\,\mathrm{cm}^{-1}$ for a 19 nm SiO₂ deposition and $333\,\mathrm{cm}^{-1}$ for 21 nm. Whereas for the constant 20 nm SiO₂ deposition the calculated g_{th} values were $979\,\mathrm{cm}^{-1}$ for 19 nm nm p-GaN etch and $962\,\mathrm{cm}^{-1}$ for 21 nm. The modal discrimination for this case was $310\,\mathrm{cm}^{-1}$ for 19 nm p-GaN etch and $405\,\mathrm{cm}^{-1}$ for 21 nm. For the nano-cylindrical apertures, varying the p-GaN etch depth results in centrally

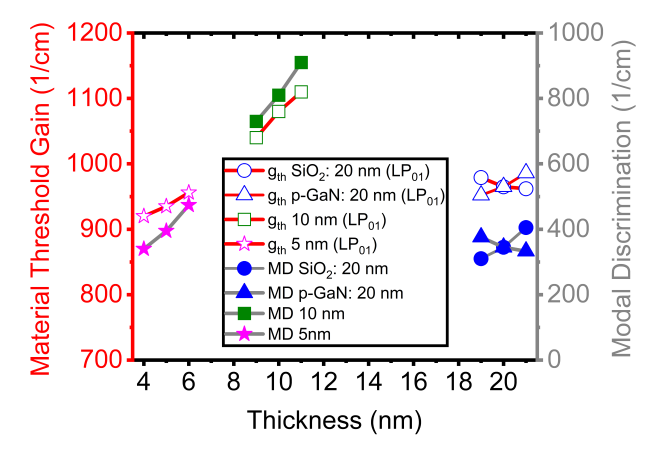


Fig. 3. Thickness vs. threshold material gain (g_{th} : left Y-axis) and modal discrimination (right Y-axis) for 4 μ m aperture structures, highlighting tolerance to fabrication variations. Etch depth variations of ± 1 nm were applied to the nano-cylindrical aperture with 5 nm and 10 nm etched p-GaN. For the buried-SiO₂ structure two cases were considered: (1) variation of the deposited SiO₂ thickness by ± 1 nm with a fixed 20 nm p-GaN etch depth, and (2) variation of the p-GaN etch depth by ± 1 nm while keeping the SiO₂ thickness constant at 20 nm.

elevated structures in all cases. And both $g_{\rm th}$ and the modal discrimination increase with increasing height of this central elevation. However, for the buried-SiO₂ structure, changing either the etched p-GaN or deposited SiO₂ thickness while keeping the other constant leads to both centrally elevated and peripherally elevated structures. We saw that the centrally elevated structure has the lower $g_{\rm th}$ values of the two. Thus, both the 5 nm nano-cylindrical design and the centrally elevated buried-SiO₂ design demonstrates strong modal selectivity, but the latter requires an additional fabrication step.

CONCLUSION

In summary, we performed simulations of InGaN-based blue VCSELs with varying aperture diameters, investigating two transverse index guiding schemes. Our results, together with those from [4,5] suggest that a modal discrimination value in the range of 300-350 cm⁻¹ is a practical benchmark for effective suppression of higher-order transverse modes. This guideline is useful for the design of mode-filtering structures such as surface reliefs, metasurfaces, or tapered oxide apertures. It is important to note that our study is based solely on optical simulations of a cold cavity. For a complete evaluation of VCSEL performance, future work should incorporate coupled optical, electrical, and thermal modeling to account for the full complexity of the device behavior.

REFERENCES

- [1] Yeh et al., Appl. Phys. Lett, 109, 241103 (2016).
- [2] Leonard et al., Appl. Phys. Lett, 108, 031111 (2016).
- [3] Kuramoto et al., Appl. Phys. Express, 12, 091004 (2019).
- [4] Kuramoto et al., Appl. Phys. Express, 13, 082005 (2020).
- [5] Terao et al., Proc. Of SPIE Vol. 11686 (2021).
- [6] G. R. Hadley, Opt. Lett. 20, 1483 (1995).